PERGAMON

Solid State Communications 111 (1999) 1–13

solid state communications

Research Paper

Electrical imaging of the quantum Hall state

A. Yacoby[†], H.F. Hess[‡], T.A. Fulton[*], L.N. Pfeiffer, K.W. West

Bell Laboratories, Lucent Technologies, 600 Mountain Ave, Murray Hill, NJ 07974, USA

Received 1 March 1999; accepted 16 March 1999 by A. Pinkzuk

Abstract

Microscopic images of the local electron compressibility, electrostatic potential, and current-induced Hall voltage of a two-dimensional sheet of electrons in the quantum Hall regime are acquired using a single-electron transistor as a scanned probe. Regions identified as differing in quantum state (Landau level) occupancy of the electrons appear in interrelated ways in all of these properties. The compressibility images show quasi-insulating "incompressible" strips, associated with edge states that bound these regions. These strips follow the contours of a constant electron density that match exact occupancy of Landau levels, and shift accordingly with magnetic field and electron density changes. The potential distribution has an overall correlation with the density contours marked by the incompressible strips and a step across the strips that provides a direct measure of the energy gap between Landau levels. The Hall voltage and the inferred current flow patterns are also guided by these strips. © 1999 Elsevier Science Ltd. All rights reserved.

Keywords: A. Heterojunctions; B. Scanning tunneling microscopy; C. Quantum Hall effect

1. Introduction

The physical properties of any macroscopic object are quantum-mechanical in origin. While this cause-and-effect relation is usually hard to see, in a few exceptional cases it is quite clear, as in the integer quantum Hall effect. Here an ordinary measurement of the current I and voltage V in a macroscopic, even though effectively two-dimensional, semiconductor device gives a ratio of I to V that is an exact multiple of the ratio of fundamental constants e^2/h, where e is the electronic charge and h Planck's constant. The same result is found over a wide range of device and experimental conditions. This quantum mechanical behavior writ large has been intensely studied since its discovery in 1980 [1]. In typical experiments, the device is a GaAs–AlGaAs heterojunction having a sheet of high-mobility electrons confined in a potential well just below the surface. At low temperatures, the electrons are restricted, in a quantum mechanical sense, to a two-dimensional motion parallel to the surface. This two-dimensional electron gas (2DEG) is subjected to a magnetic field $B > \backsim 1$ T at a low temperature, < 10 K. Four contacts on the perimeter of the 2DEG are used *alternately* as I and V terminals, and the "Hall" conductance I/V is measured as B is scanned. Whenever B approximately satisfies $B/(h/e) = n/N$, where n is the electron density and $N = 1,2,3,\ldots$, the Hall

* Corresponding author. Tel.: + 1-908-582-3463; fax: + 1-908-582-7660.

E-mail address: taf@physics.bell-labs.com (T.A. Fulton)

[†] Present address: The Weizmann Institute of Science, Rehovot, Israel

[‡] Present address: Phasemetrics Incorporated, 10260 Sorrento Valley Rd., San Diego, CA 92121, USA.

0038-1098/99/$ - see front matter © 1999 Elsevier Science Ltd. All rights reserved.
PII: S0038-1098(99)00139-8

conductance takes on the exact value Ne^2/h over a considerable range of B around this value[†,‡].

A succinct theoretical explanation of this behavior was provided shortly after the first experiments, based on a symmetry argument [2]. Since then, a more detailed picture of what happens has emerged [3]. To a first approximation, the 2DEG is a gas of non-interacting electrons confined to a plane. Owing to the large magnetic field B, these electrons occupy states of quantized cyclotron motion called Landau levels. These levels are separated in energy by gaps proportional to B. Each level can accommodate up to $B/(h/e)$ electrons/unit area. The population of the levels is described by the *filling factor* $\nu = n/B/(h/e)$. Thus, the condition of quantized conductance corresponds to an integer filling factor, meaning that the lowest N Landau levels are completely full, at low temperatures, and the rest empty[§]. This correspondence does not, however, explain the surprising persistence of the quantized conductance over a range of B and in samples of varying density, which is the essence of the quantum Hall effect. To account for this, a further concept of *edge states* [4] is required, which refers to those one-dimensional quantum-mechanical states that lie along contours of density that correspond to integer filling factors. These states have a form corresponding to the classical cycloidal motion of electrons in an $E \times B$ field, associated with current flow. Indeed one main result of the present work is to provide submicron images of the "incompressible strips" that lie along the individual edge states, subdividing the 2DEG into regions of differing Landau-level occupancy, and further to show how these strips act to guide patterns of Hall voltage and current.

The concept of edge states involves the non-uniform nature of the electron density, n. In real devices, n is depleted to zero near sample edges or biased top gates by the increase in a confining potential. Additional, less-extreme non-uniformity in n arises elsewhere from disorder in the potential, and from causes occurring in sample fabrication and treatment. Consequently, exactly integer filling factors ν do not occur everywhere at once, but only in separate, narrow regions along the contour lines of density, the edge-state contours, given by $n = NB/(h/e)$, where $N = 1,2,3,\ldots$ (Fig. 1). In the regions between the contours, the Fermi level lies within a single Landau level.

The edge state associated with $\nu = N$ will exist over a wide range of B. At low B, its contour runs in the low-n region, close to the edge. As B increases, the contour climbs in n, and eventually pulls away from the edge, following the topography of n into the interior (Fig. 1). At lower B, there are several states along the edge at once, running between the electrical contacts. This connection is lost when they move into the interior.

In a widely accepted picture, current injected at a contact tends to flow in the regions between these edge-state contours, so-called edge channels. If the contours run close to the edge, all the edge channels in proximity to one contact will provide a continuous path to a neighboring contact. It is thought that in this situation the conductance between these two contacts will show quantized behavior. If, however, the outermost contour wanders away into the interior between these contacts, the connection provided by the associated edge channel is lost and so is the quantized behavior[‖] [5].

For the older model of non-interacting electrons, an abrupt change in density n occurs at the position of an edge state, where the Fermi level crosses a Landau level. However, when the electrostatic energy is considered, the density is found to have a smoother, near-classical form (Fig. 1), except at the edge-state contours. These are marked by a narrow *incompressible strip* running along the contour [6–11]. Within this strip, the charge adjusts so that the density is fixed at $n = NB/(h/e)$ (Fig. 1), and the 2DEG is incompressible, i.e. unable to screen changes in potential, somewhat like an insulator. The relationship of the density

[†] Conductance steps are also observed, at lower temperatures, for fractional values of N, particularly for $N < 1$. These involve the more exotic fractional quantum Hall effect.

[‡] The related longitudinal resistance measured with adjacent pairs of contacts necessarily gives $V/I = 0$ over the same range. Other properties such as the specific heat and the magnetic moment also show oscillatory, but not quantized, behavior with this same pattern in B.

[§] In this case, the Fermi energy is between Landau levels, where, due to a disorder, a small percentage of the states are not Landau-like but are localized in position and not involved in conduction.

[‖] This is the net current. There are larger, oppositely flowing diamagnetic currents on the two sides, which cancel except when the Fermi levels on the two sides are unequal.

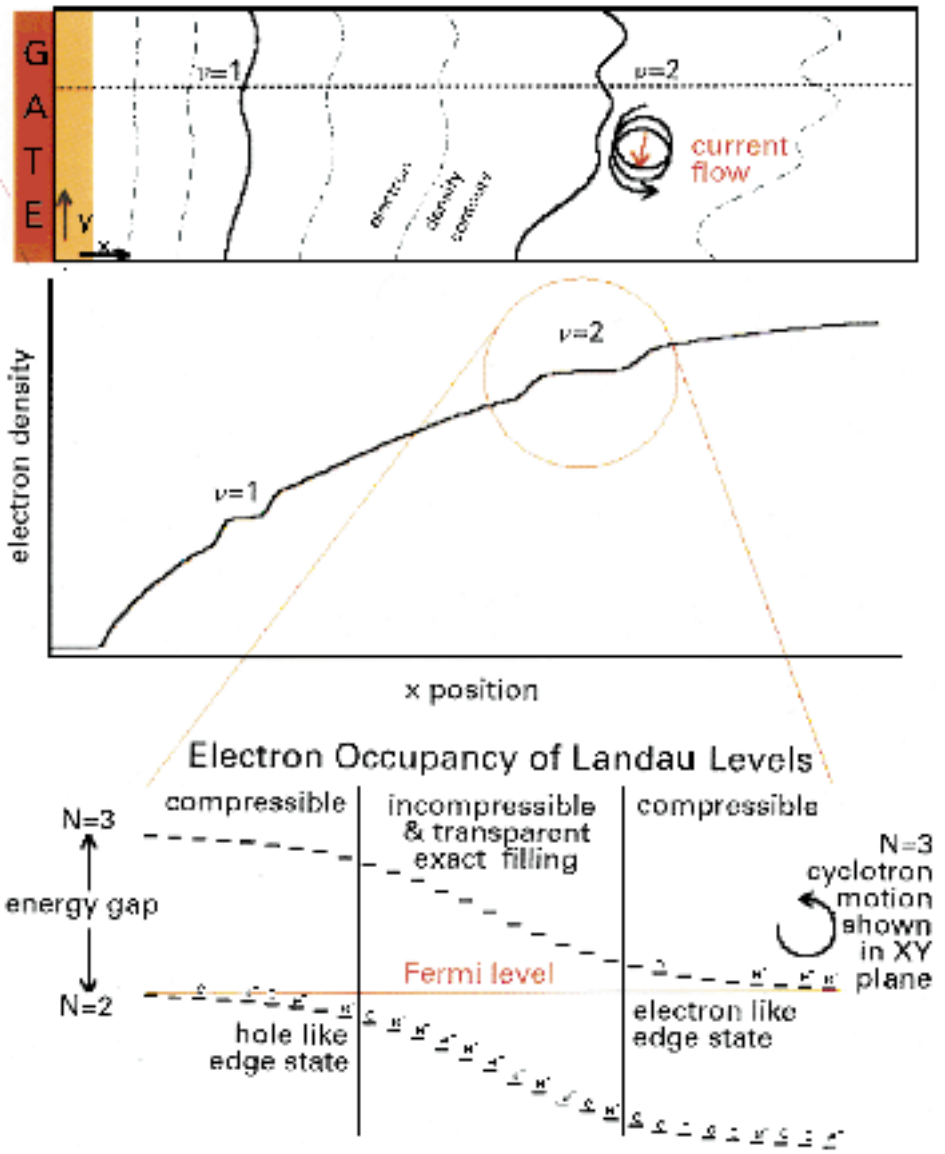

Fig. 1. Sketch of the density profile and contours of density near the edge in a somewhat non-uniform sample, with the positions of the $\nu = 1$ and $\nu = 2$ edge states and incompressible strips indicated. The edge is created by a biased gate, which induces an adjacent depleted region (orange). Insets: Regions of constant density occurring at the incompressible strips. Expanded versions of these insets (bottom) sketch how edge states, electron occupancy of Landau levels, and associated properties are expected to interrelate. An electron or "e" symbol above the dash indicates occupancy of that state. The gradual increase of electron density as one proceeds from the left to the right spans three regions: occasional vacancies for the lower Landau level; exact filling of the lower Landau level; and beginning to fill the upper Landau level. In the partly occupied regions, the 2DEG is compressible, and in the fully occupied region, it is incompressible.

profile and occupancy of Landau states and associated properties is also shown in Fig. 1. In the two regions adjacent to the strip, the electrons reside in partly-filled N or $N + 1$ Landau levels and the 2DEG is compressible, i.e. n can adjust to screen potential variations. The movement of charge that creates the strip is driven by the energy gap between these levels, similar to what occurs in a pn junction. This causes a

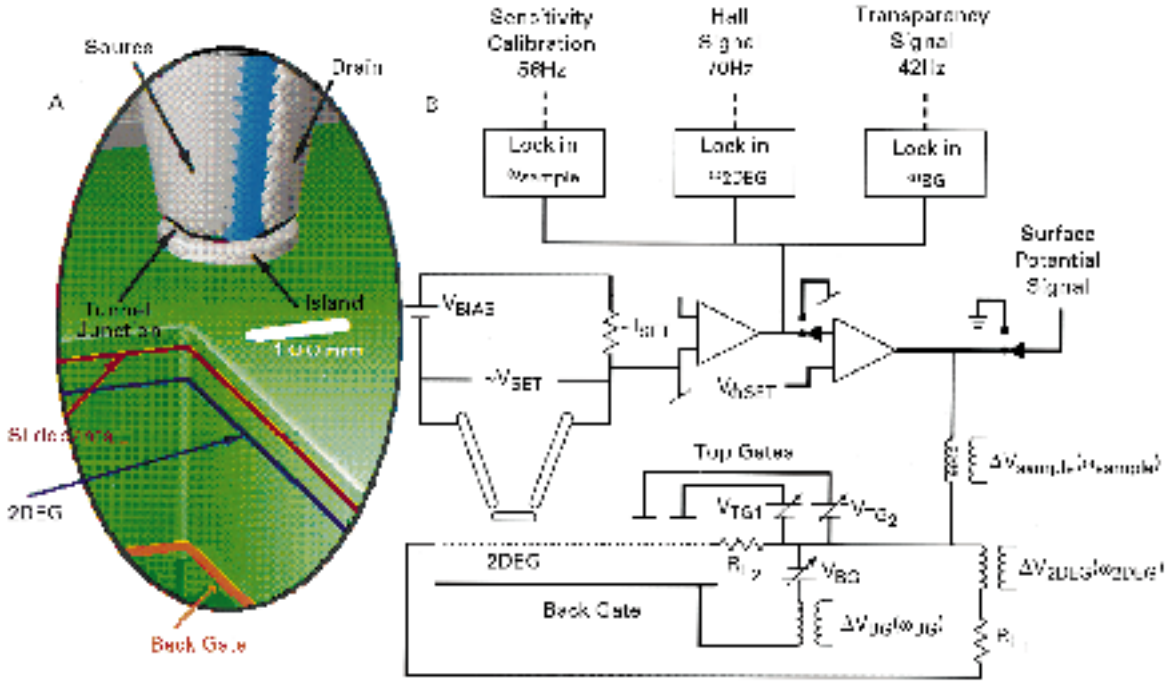

Fig. 2. (A) Sketch of the SET probe suspended over the GaAs/AlGaAs heterostructure. The 2DEG is formed below the silicon dopants and above a deeper (by $\backsim$ 5 μm) back gate. (B) Schematic of the circuit of the SET bias, feedback and modulation electronics. A simple voltage-source plus-resistor circuit biases the SET to a voltage $\backsim V_{SET}$ and a current $\backsim I_{SET}$. The variations of I_{SET} as sensed by the resistor are amplified and form the signal output. Three different lock-in amplifiers can record the transparency, Hall effect and calibration signals, simultaneously. A switch also allows direct measurement of the electrostatic potential by feedback of the signal to hold the SET current constant. The $V_{\phi SET}$ voltage is used to offset the tip vs. sample voltages such that potentials induced by work-function differences are minimized.

step in work function equal to this gap to appear across the strip.

With direct imaging of the spatial structure of the quantum Hall effect, one can confirm critical assumptions of current theoretical models and clarify how microscopic details influence the more standard macroscopic conductivity measurements. The older, related question of whether the Hall voltage and transport current are confined to the edge of the sample or distributed uniformly in the quantized regime similarly lends itself to imaging. Many interesting results have already been obtained in these directions, variously using multiple contacts [12], local heating [13], Pockels effect [14], breakdown [15], differential lateral photoeffect [16–18], and inductive probing [19]. Most recently elegant work-function measurements have been made with a fixed single-electron transistor (SET) [20]. Also, intriguing detailed scanned images of $\backsim$ 100 kHz charge accumulation phenomena involving the electron compressibility and resistivity in the quantum Hall regime have been obtained [21]. Finally, Hall voltages have been imaged with good sensitivity on a fine scale using a scanning electric-force probe [22] operated at $\backsim$ 100 kHz.

In what follows a SET scanning electrometer [23] is used to map out, concurrently, three related properties of a 2DEG in the quantum Hall regime. These are the electrostatic surface potential V_{surf}, which is directly related to the work function and hence to dopant ionization and to the electron density, the “transparency” of the 2DEG to the electric field from a back gate, which probes the electron gas compressibility, and the voltage, primarily a Hall voltage, induced by transport current. The incompressible strips associated with edge states show up in related ways in all these images, especially the transparency, where they allow us to map out the 2DEG electron density. An

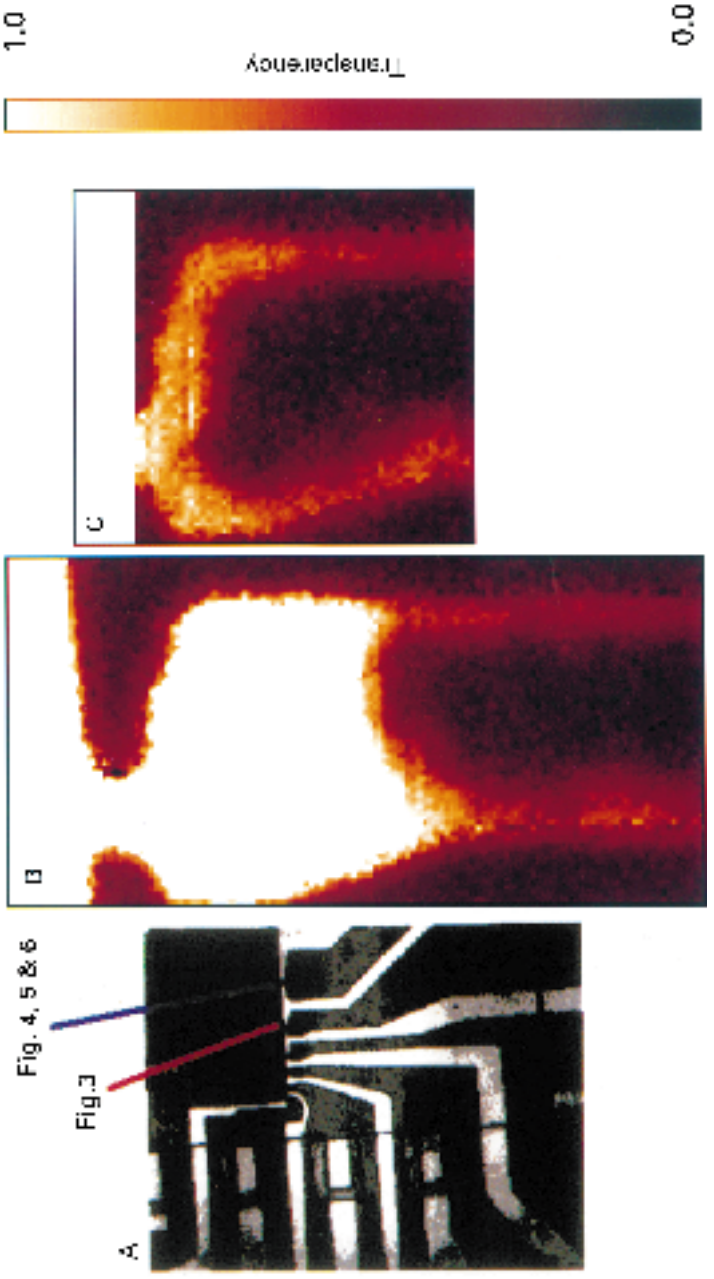

Fig. 3. (A) Micrograph (70 × 110 μm) of the patterned sample showing seven top gates overlapping the 2DEG, which occupies the upper and center-right region. Ohmic contacts to the 2DEG are interspersed between the gates. (B) and (C) show 5 × 15 μm and 5 × 5 μm transparency images of depleted 2DEG regions (in arbitrary units) for top-gate biases of −0.4 and −0.1 V, respectively.

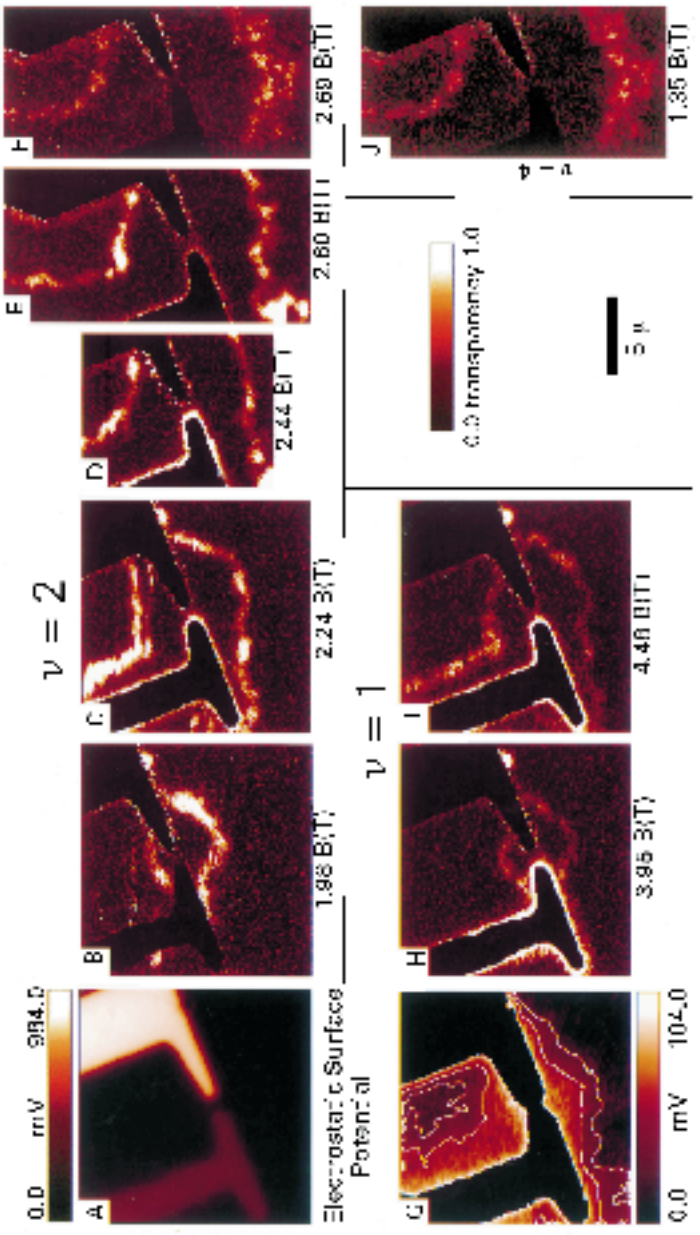

Fig. 4. (A) Typical electrostatic potential, or V_{surf} image, on a 1.0 V scale, of the sample showing the left and right gates, for $B = 4.48$ T. Such images are obtained concurrently with each transparency image, but do not change noticeably on this scale. (B–F, H, I and J). Transparency images for different magnetic fields around filling factors of $\nu = 2$, 1 and 4. The transparency, shown in arbitrary units, is a measure of screening of the modulated back-gate voltage see page 10, footnote [‡]. (G) The electrostatic potential of (A) shown with $\sim \times$ 10 higher sensitivity with two contour lines. The black masks in the figure and Fig. 5 outline the position of the gates. The weak signals seen at the gate edges in the transparency images are due to limitations of the scanning SET electronics in steep voltage gradients. Some images also show the effect of a small ac voltage component at the back-gate frequency on the left gate.

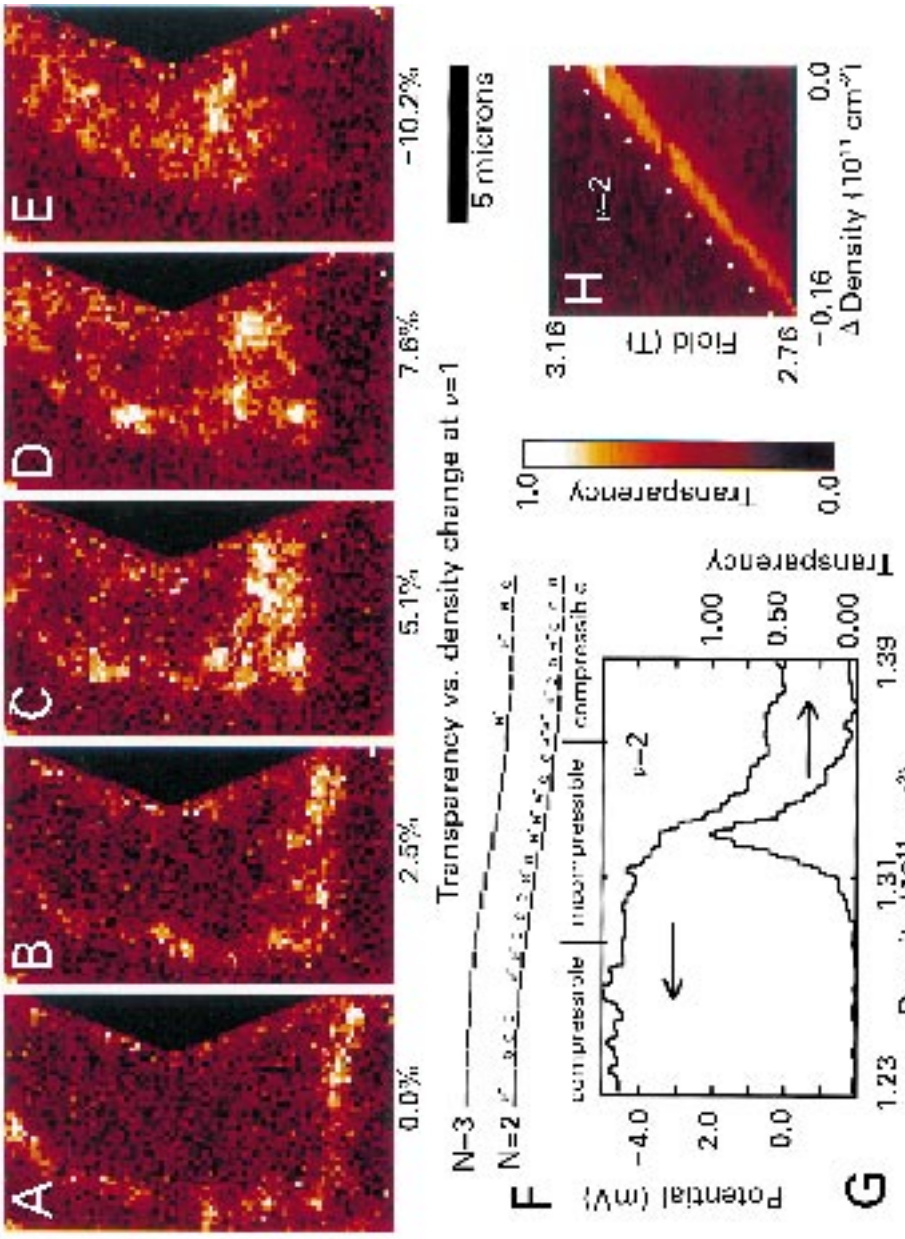

Fig. 5. (A)–(E) A transparency sequence at $B = 5.2$ T in which the back gate is employed to decrease the density by $\sim 1.3 \times 10^{10}$ electrons/cm^2. The incompressible strips here are for $\nu = 1$. (F) A sketch showing how electrons fill the available Landau level states as in Fig. 1. It is a guide to the data of (G). (G) Data showing the potential step and corresponding transparency signature created by passing a strip under the SET (held at a fixed point) by decreasing density with the back gate. (H) Color-scale plot showing the transparency signal vs. the back-gate-induced density change and the magnetic field at a fixed point. This shows the locus of magnetic field vs. electron density for which the transparency strip does not shift. The expected slope, indicated by the dotted line, is h/Ne with $N = 2$ for the second Landau level.

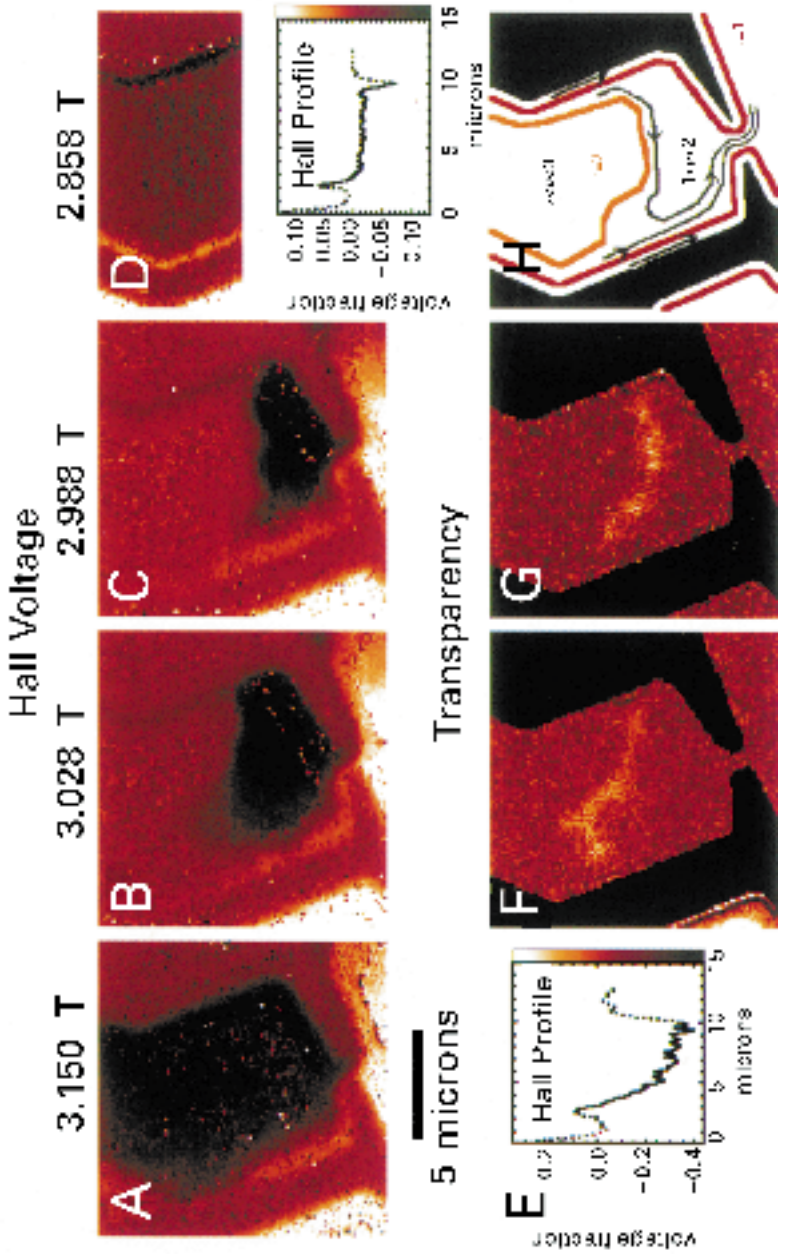

Fig. 6. (A)–(D) Image of the voltage induced in the sample by an applied current under a range of magnetic fields near $\nu = 2$. The Hall voltage appears roughly linear at the highest field (A), but becomes increasingly non-linear as the field decreases (B)–(D). Corresponding transparency images (F) and (G) show how the current flow interacts with the incompressible strip and forms the patterns sketched in (H). These current flow vectors are inferred from the spatial gradient in the Hall potential. These data were taken in a separate cool-down from those of Figs. 4 and 5.

extensive study of the field and density dependence, and the interrelation of all three imaged quantities gives a cohesive physical picture of the quantum Hall effect, whereby the distribution of dopant ionization, electron density, Landau level occupancy and current flow can be understood in unison.

2. The experimental system

In our GaAs/AlGaAs heterojunction sample, a 2DEG forms on the GaAs side of the interface, 100 nm below the surface (Fig. 2(A))[†]. Silicon dopants in the upper part of the AlGaAs supply electrons both to states at the surface and to the 2DEG[‡,§]. Several metal gates (TiAu) are patterned on the surface (Fig. 3(A)). These enable us to deplete the 2DEG and to restrict current flow to specific regions. Additionally, a back gate is formed by a 1 μm thick $n+$ layer, 5.4 μm below the 2DEG, allowing us to decrease and/or modulate the electron density. The data of Figs. 4–6 are obtained from our main sample, whose mobility was 4×10^6 cm^2/V s, before patterning, and in which the range of density, measured locally with the SET probe, is $0.8–1.25 \times 10^{11}$ electrons/cm^2. This sample showed the usual quantized conductances, which occurred at fields corresponding to somewhat larger densities. The data of Fig. 3 came from a second sample of the same physical configuration, but of a lower density, estimated as $\backsim 4 \times 10^{10}$ electrons/cm^2.

The combination of good electrostatic sensitivity at d.c. and low frequency ($< 100\,\mu$V/Hz$^{1/2}$) at $<$ 100 Hz, which minimizes resistive effects, and sub-micron resolution necessary for the present experiments is obtained by using a SET[‖] [24,25] as a scanning electric field probe (Fig. 2(A)). It is fabricated on the flat, $\backsim$ 100 nm diameter tip of a tapered glass fiber, which hovers $\backsim$ 100–200 nm above the sample surface[¶]. Any changing potential under the probe modulates the current through the SET. By monitoring this current while scanning the probe in a raster pattern across the surface, one can construct "electric-field" images of $V_{\rm surf}$, which is a measure of the electric-field flux emanating from the surface [23]. For the most part this is accomplished with a sample voltage feedback ($V_{\rm b} = -V_{\rm surf}$) that nulls any SET response (Fig. 2(B)). To extract the mV-level transparency and transport signals from the large static signals of biased surface gates ($\backsim$ 1 V) and fluctuating surface and dopant charges ($\backsim$ 50 meV) [23], we use low-frequency modulation and lock-in detection schemes (Fig. 2(B)). For the transport signals, an a.c. current δI is passed through the 2DEG and the induced voltage, $\delta V_{\rm surf}$, is measured, giving $\delta V_{\rm surf}/\delta I$. Similarly an a.c. back-gate voltage $\delta V_{\rm BG}$ that leaks through the 2DEG and is not fully screened gives the transparency signal, $\delta V_{\rm surf}/\delta V_{\rm BG}$. This transparency signal is related to the compressibility κ of the 2DEG by $\delta V_{\rm surf}/\delta V_{\rm BG} = C/e\kappa$, where C is the capacitance between the 2DEG and the back gate [26,27]. Apparent transparency signals can also arise if the resistance of the current paths in the 2DEG is so large that the charging of an area is not able to follow the a.c. gate voltage. As described later, we sometimes see out-of-phase or unusually-large signals that we ascribe to this cause, but most of the transparency features appear not to involve resistive effects.

3. Low-field transparency

An example of transparency measurements at zero applied magnetic field is given in Fig. 3. The micrograph of Fig. 3(A) shows a set of top gates overlapping the nominally uniform 2DEG. The SET is raster-scanned across the area indicated by the red line. Any signal penetrating the 2DEG from an a.c. back-gate voltage is recorded. Two representative color-scale images of these signals appear in Fig. 3(B) and (C). These correspond to different top-gate biases. Regions of large signal (white) occur where the back gate is unscreened because the 2DEG is fully

[†] Since the 2DEG is buried by $\backsim$ 100 nm, the apparent width of 2DEG features exceeds that of surface features by $\backsim$ 200 nm.

[‡] The density of 2DEG negative charge is equal to the net positive charge density in the donor layer and the surface.

[§] Measurements are made in the dark to avoid the formation of a parallel conduction in the donor layer.

[‖] The signal levels here correspond to $\backsim 0.01e/0.001e$ induced on the SET island at dc/low frequency a.c.

[¶] Tip size and heights are estimated from the capacitance and the observed spatial resolution. In most images, surface features such as gate edges are $\backsim$ 600 nm wide. All conductors on the sample are given a common bias offset relative to the tip of $\backsim -0.8$ V to roughly cancel the work-function difference between the 2DEG and the tip, so as to minimize the charge induced by the tip. Measurements are made at a temperature of $\backsim$ 0.8 K.

depleted by the fringing fields of the top gates. The areas of no signal (dark red) occur where the back gate is screened, either in conducting areas where the 2DEG is not fully depleted or over the T-shaped metal gates. Areas of intermediate color and signal level next to the gates are unresolved, narrow depleted regions caused by the gate bias [9]. These signals increase in strength and coverage as the gate bias is made more negative, and eventually cover the entire area between the gates. The non-uniform depletion in this region shows, qualitatively, that the density here is also non-uniform. Note that when areas near the constriction are fully depleted, an open circuit would result in a contact-based measurement.

4. Transparency and surface potential in the quantum Hall regime

Clear-cut microscopic structure arising from the incompressible strips appears in the images of the transparency presented in Figs. 4 and 5. These are obtained from our main sample in the region shown by the blue line in Fig. 3(A), and cover a range of magnetic fields corresponding to filling factors from 1 to 4. For orientation, a typical image of the V_{surf} in this region is shown in Fig. 4(A), and on an expanded scale in Fig. 4(G). Here the gates show up against the 2DEG background owing to their different work functions and their biases, 0 and -0.6 V for the left- and right-hand gates. The electron density under and just adjacent to the latter gate is depleted to zero by the bias, forming an edge to the 2DEG.

The transparency images of this region (remaining panels of Fig. 4) reveal compressible and incompressible phases of the 2DEG. The upper row (Fig. 4) corresponds to magnetic fields near $\nu = 2$[†]. These show regions of strong signal (lighter colors) where the a.c. bias of the back gate penetrates the 2DEG. The regions appear as isolated, non-uniform strips that meander across the image. In the rest of the region, there is no signal (dark red) as the 2DEG screens the back gate. By definition, the regions of signal are incompressible areas of 2DEG surrounded by compressible areas. The strips shift with increasing magnetic field, and, allowing for some drift and hysteresis, form a pattern resembling contour lines. Based on this, and the overall behavior described below, we identify these as the incompressible strips that lie along the $\nu = 2$ edge states, marking the contours of electron density that correspond to the filling $\nu = n/B/(h/e) = 2$. Similar strips of the same general shape are observed at double and half the magnetic field, and correspond to the $\nu = 1$ and $\nu = 4$ states (Fig. 4(H)–(J))[‡,§].

One expects these strips to lie not just in the open areas, but as much or more so near the edge of the 2DEG, along the right-hand gate (shown masked). If these strips are too close to the gate, however, then the signals are screened by the gate metal and cannot be seen with our present sensitivity. Thus, where a strip appears to run into the gate (e.g. Fig. 4(B) and (C)), it actually turns and runs along it, invisibly. These strips do become visible once B increases to the point that the contour draws away from the gate, as in the series of Fig. 4(D)–(F).

From the shapes of these strips and the range of B over which they occur, it follows that the electron density is non-uniform, having a large, unexpected depression centered near the constriction. The specific densities on each contour are given by the $\nu = 2$ condition, and range from $\backsim 8 \times 10^{10}$ to $\backsim 1.25 \times 10^{11}$ electrons/cm^2. The depth of this depression turns out to roughly follow the gate bias, but its width far exceeds the usual depletion length. It is probably caused by a slight leakage of charge onto the surrounding surface.

Considerable structure, probably due to fluctuations in the density, occurs in all the strip images. In places there are bright blobs, apparently regions isolated by closed loops. Unlike most of the signals, which are in

[†] The exact density is unknown a priori, but can be estimated from the Hall conductance and voltage required for depletion under the gates. Comparison of the strip movement with B and back-gate voltage, described below, confirms the $\nu = 2$ identification.

[‡] The transparency signal is a measure of the 2DEG compressibility, but the relation is complex for an incompressible strip structure, so here we do not attempt a quantitative extraction of the compressibility. The strength of the signal for the $\nu = 1$, 2 and 4 strips scales roughly with the size of the associated energy gaps, consistent with the signal being primarily due to the induced ac motion of the potential step at the strip.

[§] Weak signals were observed for $\nu = 6$, but not $\nu = 3$ or 5. The signals for even ν should scale with B, and be strong compared to those for odd ν. The signal for $\nu = 3$ should be $\backsim 1/9$ that for $\nu = 1$.

phase with the a.c. gate voltage, the signals in these larger blobs show a decided phase lag, even at 42 Hz, indicating that the strips are quite resistive, particularly those for $\nu = 2$[†].

A negative bias of the back gate causes a decrease of electron density, n, that moves the strips much like an increase in B. The set of transparency images in Fig. 5(A)–(E) shows how some $\nu = 1$ strips change as n is reduced by about 10%. In fact the filling can be quantitatively identified by the relative sensitivities to n and B, as shown below in regard to Fig. 5(H).

A step in surface potential occurs at each strip, corresponding to the energy gap between the Landau levels on either side (see Fig. 5(F)). These steps are observed in potential images, but they are best measured by holding the SET tip fixed and passing the incompressible strip underneath it, using the back-gate voltage. Fig. 5(G) shows such a plot of V_{surf} vs. V_{BG} for a $\nu = 2$ strip. The step is $\backsim$ 4.5 mV, near the expected value, given by the cyclotron energy $h\omega_c/2\pi$, of 1.7 meV/T. Across the $\nu = 1$ strip, at twice the field, a smaller gap $\backsim$ 2 mV is measured, consistent with the expected exchange-enhanced Zeeman spin splitting energy of 0.35–0.5 meV/T[‡] [28]. Fig. 5(H) is a color-scale image of 50 such transparency scans, covering a range of B, for a strip believed to correspond to $\nu = 2$. As expected, the position of transparency peak falls on a straight line whose slope corresponds to the relation $n/B = 2/(h/e)$.

There is a clear large-scale correlation between the incompressible strips seen in transparency and the surface potential. In the V_{surf} image of Fig. 4(G), there is a region of decreased V_{surf} around the constriction, which matches the depression in density. The two contours of V_{surf}, 20 mV apart, resemble in detail the shapes of the transparency strips in these areas. We believe that an excess negative charge, injected by the biased gate, resides near the surface in this region. Its image charge in the 2DEG creates the depression in n, and the dipole layer thus formed reduces the surface potential. A surface charge density of, say, 1×10^{10} electrons/cm^2 would deplete the 2DEG by this amount, and would decrease V_{surf} by $\backsim$ 15 mV. Depressions in n and V_{surf} of these proportions are roughly what are observed.

Could these transparency signals arise from the high resistances that occur in the quantum Hall regime, rather than from the local compressibility? To review, from the magnetic-field and density dependence, it is evident that the transparency strips lie along the edge-state contours of density. A step in work function occurs at the same location. Except for the bright blobs, the signals have amplitudes consistent with this step and are in phase with the applied a.c. voltage. Owing to the substantial gradients in density, the regions leading up to the strips are not highly resistive. In similar measurements, not shown here, carried out when the top-gate bias is removed, the density gradients are comparatively small, and the transparency signals do show considerably more large-amplitudes, out-of-phase behavior over larger areas, which we associate with non-equilibrium charging of the 2DEG.

5. Hall voltage and current in the quantum Hall regime

The applied current at high B fields flows primarily as Hall current driven by the accompanying transverse, or Hall, voltage gradient. Classically, in a uniform sample, this flow would be uniform, and the Hall voltage would drop linearly across the sample. This is indeed observed at low magnetic fields. In the quantum Hall regime, however, the current and voltage drop are thought to be somewhat concentrated near the edges, flowing there via *edge channels* [29–35]. These are areas bounded by adjacent incompressible strips, e.g. by the $\nu = 1$ and $\nu = 2$ strips. In a uniform sample, these lie primarily along the edges. If an edge channel runs the length of the current path, in theory it contributes exactly e^2/h to the total Hall conductance, and so would carry that part of the applied current, and support a voltage drop in proportion[§] [5]. There still remains an

[†] In a typical case we estimate a resistance of $\backsim 10^{15}\ \Omega$ across a loop 10 μm long.

[‡] The change in density needed to cross the step is $\backsim 3 \times 10^9$ electrons/cm^2, which sets a limit on the number of localized states in the $\nu = 2$ gap [20] at this location.

[§] A particular edge channel may occur on both sides of the 2DEG strip. A total quantized conductance e^2/h is contributed by the two sides. The division of currents and voltage depends upon the details of the current injection by the contacts.

active discussion, however, as to when and to what degree the current is concentrated at the edges.

The sequence of images of Fig. 6 shows how the voltage is distributed in this sample in the magnetic field region near $\nu = 2$. Here, the two gates are biased to depletion, and an applied a.c. (70 Hz) current flows down the 2DEG between them, exiting through the constriction. The resultant a.c. voltage, measured by the SET, is primarily a transverse Hall voltage drop across the 2DEG. Its required magnitude from edge to edge is the current, $\backsim 0.4$ mA, divided by the Hall conductance, $\backsim 13\ \mathrm{k}\Omega$. The first image of the Hall voltage drop (Fig. 6(A)), and its profile across the 8 μm wide 2DEG strip (Fig. 6(E)), show a monotonic, roughly linear decrease across the strip. Over the next three images, which cover a 10% decrease in B, the voltage drop becomes concentrated at the edges (Fig. 6(D))[†]. The intermediate fields (Fig. 6(B) and (C)) show both behaviors, the voltage drop being distributed in the lower part and concentrated at the edges in the upper part. The dividing line is marked with an incompressible strip, probably that for $\nu = 2$, as seen in the concurrent transparency images of Fig. 6(F) and (G).

In these images the measured voltage drop falls much below the required total of $\backsim 4.2\ \mathrm{mV} = (0.4\ \mathrm{mA} \times 13\ \mathrm{k}\Omega)$, by up to $\times 4$ in Fig. 6(D) and $\times 2$ in Fig. 6(A) and (E). This "missing" voltage drop must occur close ($< \backsim 0.5$ μm) to the edges of the 2DEG, since only there, where the signals are largely screened by nearby gates, would the SET be unable to detect so large a drop. Thus, in Fig. 6(D) the two peaks at the edges are the screened versions of steps some $5\times$ higher. Similarly, in Fig. 6(A) the missing 50% of the voltage drop must occur at the edges as steps. The same holds for Fig. 6(B) and (C).

Given the location of the $\nu = 2$ strip in Fig. 6(F) and (G), it appears that the two incompressible strips for $\nu = 1$ and $\nu = 2$ both run along the edges of the 2DEG in Fig. 6(D). Hence there are two edge channels, the 1–2 between the strips and the 0–1 between the $\nu = 1$ strip and the edge of the 2DEG. These two channels contribute $2e^2/\mathrm{h}$ to the Hall conductance, accounting for most of the total near $\nu = 2$. This is in accord with the concentration here of the voltage drop, and hence the current at the edges.

In contrast, in Fig. 6(A) and (E) there is only the 0–1 channel, the $\nu = 2$ strip having been removed. Here, the total Hall conductance and the voltage drop have changed little, since the field increase is small, $\backsim 10\%$. Now, however, half the voltage drop is spread across the central region. The remaining half occurs at the edge, probably at the 0–1 channel, whose conductance is half the total. The currents would divide in the same way.

In this sequence, the constriction and the region just above may be viewed as forming a current contact. The change in behavior that occurs between when the $n = 2$ strip enters the contact and when it does not is illustrative of the manner in which conductance quantization is thought to depend on the edge-state positions. The drawing (Fig. 6(H)) shows schematically the location of the regions of different filling factor ν and the current flow deduced from the transparency and the Hall voltage images of the two intermediate fields. It illustrates how current flow is redistributed when the incompressible strip for $\nu = 2$ peels away from the edge.

The simultaneous imaging of the electrostatic potential, transparency, and Hall voltage with the SET has revealed the local electron density, shown complex structure of varying Landau level fillings in the quantum Hall state, and has provided a qualitative picture of the current flow on a microscopic scale. Further modeling and analysis of such data should provide information on properties such as the local mobility and the Hall angle, and yield a quantitative measure of the current flow. A detailed comparison of contact-based and SET Hall voltage measurements in closer proximity would be interesting. Images with higher spatial resolution would permit measuring the structure of the incompressible strips in more detail. Higher voltage sensitivity combined with higher magnetic fields and lower temperatures would allow one to image the more exotic fractional quantum Hall effect ($\nu =$ simple rational fraction) with its smaller gap voltages [36,37]. Given that the Landau levels have spin polarization, there might even be a means to measure microscopic magnetization effects in the 2DEG. Overall, such imaging techniques can reveal

[†] The image in panel D did not include the constriction region. Judging from other images in this region, the purely edge-concentrated voltage drop may or may not have extended to the constriction. The discussion is unaffected by this.

the complex structure of two-dimensional systems that underlie the contact-based conductivity measurements.

Acknowledgements

We thank A. Stern, B.I. Halperin, A.L. Efros, A.M. Chang, R.L. Willett, S.H. Simon, S. He, C.M. Varma and N. Zhitenev for very useful discussions. We received experimental help from K.W. Baldwin, R.J. Chichester, and L.N. Dunkleberger.

References

[1] K. von Klitzing, G. Dorda, M. Pepper, Phys. Rev. Lett. 45 (1980) 494.
[2] R.B. Laughlin, Phys. Rev. B 23 (1981) 5632.
[3] T. Chakraborty, P. Pietilainen (Eds.), The Quantum Hall Effects: Integral and Fractional Solid State Sciences, 85, Springer, New York, 1995.
[4] B.I. Halperin, Phys. Rev. B 25 (1982) 2185.
[5] M. Buttiker, Phys. Rev. B 38 (1988) 9375.
[6] A.L. Efros, Solid State Comm. 67 (1988) 1019.
[7] C.W.J. Beenakker, Phys. Rev. Lett. 64 (1990) 216.
[8] A.M. Chang, Solid State Comm. 74 (1990) 871.
[9] D.B. Chklovskii, B.I. Shklovskii, L.I. Glazman, Phys. Rev. B 46 (1992) 4026.
[10] B.E. Kane, Ph.D. thesis, Princeton University, NJ, 1988.
[11] D.B. Chklovskii, P.A. Lee, Phys. Rev. B 48 (1993) 18060.
[12] G. Ebert, K. von Klitzing, G.J. Weimann, Phys. C: Solid State Phys. 18 (1985) L257.
[13] U. Klass, W. Dietsche, K. von Klitzing, K. Ploog, Physica B 169 (1991) 363.
[14] P.F. Fontein, J.A. Kleinen, P. Hendriks, F.A.P. Blom, J.H. Wolter, H.G.M. Lochs, F.A.J.M. Driessen, L.J. Giling, C.W.J. Beenakker, Phys. Rev. B 43 (1991) 12090.
[15] N.Q. Balaban, U. Meirav, H. Shtrikman, Y. Levinson, Phys. Rev. Lett. 71 (1993) 1443.
[16] R.J.F. van Haren, F.A.P. Blomand, J.H. Wolter, Phys. Rev. Lett. 74 (1995) 1198.
[17] R. Knott, W. Dietsche, K. von Klitzing, K. Eberl, K. Ploog, Semicon. Sci. Tech. 10 (1995) 117.
[18] A.A. Shashkin, A.J. Kent, J.R. Owens-Bradley, A.J. Cross, P. Hawker, M. Henini, Phys. Rev. Lett. 79 (1997) 5114.
[19] E. Yahel, D. Orgad, A. Palevski, H. Shtrikman, Phys. Rev. Lett. 76 (1996) 2149.
[20] Y.Y. Wei, J. Weis, K. von Klitzing, K. Eberl, App. Phys. Lett. 71 (1997) 2514.
[21] S.H. Tessmer, P.I. Glicofridis, R.C. Ashoori, L.S. Levitov, M.R. Melloch, Nature 392 (1998) 51.
[22] K.L. McCormick, M.T. Woodside, M. Huang, M. Wu, P.L. McEuen, C.I. Duruoz, J.J. Harris, cond-mat/9811143, in press.
[23] M.J. Yoo, T.A. Fulton, H.F. Hess, R.L. Willet, L.N. Dunkleberger, R.J. Chichester, L.N. Pfeiffer, K.W. West, Science 276 (1997) 579.
[24] T.A. Fulton, G.J. Dolan, Phys. Rev. Lett. 59 (1987) 109.
[25] D. Averin, K.K. Likharev, J. Low Temp. Phys. 62 (1986) 345.
[26] J.P. Eisenstein, L.N. Pfeiffer, K.W. West, Phys. Rev. B 50 (1994) 1760.
[27] S. Shapira, U. Sivan, P.M. Solomon, E. Buchstab, M. Tischler, G. Ben Yoseph, Phys. Rev. Lett. 77 (1996) 3181.
[28] E.E. Mendez, J. Nocera, W.I. Wang, Phys. Rev. B 47 (1993) 13937.
[29] A.M. MacDonald, T.M. Rice, W.F. Brinkman, Phys. Rev. B 28 (1983) 3648.
[30] D.J. Thouless, J. Phys. C: Solid State Phys. 18 (1985) 6211.
[31] D. Pfannkuche, J. Hajdu, Phys. Rev. B 46 (1992) 7032.
[32] I.M. Ruzin, Phys. Rev. B 47 (1993) 15727.
[33] C. Wexler, D.J. Thouless, Phys. Rev. B 49 (1994) 4815.
[34] S. Komiyama, H. Hirai, Phys. Rev. B 54 (1996) 2067.
[35] K. Tsemekhman, V. Tsemekhman, C. Wexler, D.J. Thouless, Solid State Commun. 101 (1997) 549.
[36] J.J. Palacios, A.M. MacDonald, Phys. Rev. B 57 (1998) 7119.
[37] J. Shiraishi, Y. Avishai, M. Kohmoto, cond-mat/9710309, unpublished.